

Social Zone as a Barrier Function for Socially-Compliant Robot Navigation ^{*}

Junwoo Jang ^{*} Maani Ghaffari ^{*}

^{*} *Department of Naval Architecture and Marine Engineering
University of Michigan, Ann Arbor, MI 48109, USA
e-mail: {junwoo, maanigj}@umich.edu*

Abstract: This study addresses the challenge of integrating social norms into robot navigation, which is essential for ensuring that robots operate safely and efficiently in human-centric environments. Social norms, often unspoken and implicitly understood among people, are difficult to explicitly define and implement in robotic systems. To overcome this, we derive these norms from real human trajectory data, utilizing the comprehensive ATC dataset to identify the minimum social zones humans and robots must respect. These zones are integrated into the robot’s navigation system by applying barrier functions, ensuring the robot consistently remains within the designated safety set. Simulation results demonstrate that our system effectively mimics human-like navigation strategies, such as passing on the right side and adjusting speed or pausing in constrained spaces. The proposed framework is versatile, easily comprehensible, and tunable, demonstrating the potential to advance the development of robots designed to navigate effectively in human-centric environments.

Keywords: Social Navigation, Social Interaction Space, Human-robot Interaction, Control Barrier Function, Safety Control

1. INTRODUCTION

Robots are designed as intelligent systems to assist humans by taking over dangerous or repetitive tasks. Socially assistive robots, for example, aid in household chores at home and guide visitors in large public spaces like museums and airports (Fu et al., 2023; Kathuria et al., 2022). These robots are becoming increasingly integrated into our daily lives, enhancing comfort and efficiency. As robots and humans coexist, it is essential for robots to inherently possess the capability to navigate toward their destinations while avoiding people and obstacles in human-centric spaces.

Beyond simply avoiding physical collisions, robots must adhere to social norms by moving like humans. For example, we often walk on the “right” side of a path or maintain a respectful distance from others. Similarly, robots should know how to navigate human environments in a socially compliant and culturally aware manner. This capability is studied within a research field known as social navigation. Many studies on social navigation are underway, yet evaluating and employing them is challenging due to the diversity of scenarios (Mavrogiannis et al., 2023; Francis et al., 2023). There are many possible scenarios, such as navigating narrow paths, avoiding a group of people, or following a specific person, with diverse costs like collision safety, human comfort, robot politeness, and legibility. Therefore, algorithms and frameworks need to be developed in a form that easily accommodates these extensions.

Proximity is a classic and universally applicable factor that explains avoidance movements around people (Svenstrup et al., 2010). Humans naturally maintain certain distances from each other. Research on modeling various proxemics, or **social zones**, explores the personal space around individuals, which,

if invaded, can cause discomfort (Rios-Martinez et al., 2015). This field was initially defined as concentric circular zones around a person (Hall, 1963), representing different levels of comfort. Later models introduced more complex shapes, such as egg-shaped zones emphasizing the importance of frontal space (Hayduk, 1981; Kirby et al., 2009) or asymmetrical with smaller spaces on the pedestrian’s dominant side (Wkas et al., 2006; Gérin-Lajoie et al., 2008). Further studies have shown that personal spaces can be dynamic, depending on factors like speed or grouping (Truong and Ngo, 2016; Negggers et al., 2022b), and people might have different social zones with robots (Patompak et al., 2020). Traditionally, these social zones have been identified through experimental settings. The size and nature of social zones can vary significantly depending on several aspects, including the surrounding environment, the density of people present, cultural norms, and regional differences.

To study natural human behavior, it is essential to investigate social zones based on data recorded from real human data. Recently, Corbetta et al. (2018) and Pouw et al. (2024) investigated how people maintain distance and avoid each other by recording and analyzing the trajectories of pedestrians in real life. However, when using natural human data, we have to consider that individuals may have different policies because they may perceive social zones differently, and sometimes they do not strictly respect others’ social zones. With this in mind, we aim to learn about the minimum social zone, which must always be strictly adhered to for robots.

Once social zones are learned from real-life data, we can develop socially compliant movement behaviors using the control-barrier function (CBF) (Ames et al., 2019). We regard the social zone as hard constraints that should not be breached, and CBF ensures that the robot always stays within a safe set.

^{*} This research was supported by NSF Award No. 2118818.

To respond to dynamic pedestrians, we employ model predictive control (MPC) combined with CBF (Teng et al., 2021; Zeng et al., 2021), which considers the future within a given prediction horizon.

We demonstrate that our method can adhere to social norms across diverse scenarios. To the best of the author’s knowledge, this is the first attempt to derive social zones from real-life data and apply this insight to robot control, enabling robots to exhibit behaviors that closely mimic human interactions.

2. LEARNING SOCIAL ZONE

When robots move to avoid humans, it is important to ensure not only physical safety, which prevents collisions but also psychological safety, which avoids causing disturbance or discomfort to people. People maintain a respectful distance from each other while passing by, preemptively taking actions to signal their intent not to intrude into personal space. Although the social zones formed through interactions in various situations are not defined by explicit rules, they are universally recognized and practiced. To quantify the social zone, research has been conducted where robots move at different speeds and angles, investigating the comfort levels perceived by people (Neggers et al., 2022a). However, psychological studies within a laboratory setting may differ from actual human behavior, and there is an issue that these studies do not mimic all possible situations, nor do they accommodate the varying levels of comfort unique to each individual.

In this regard, we analyze the actual pedestrian trajectories to quantify the social zone. Pedestrian trajectory data has been crucial for prediction problems and is therefore publicly accessible (Korbmacher and Tordeux, 2022). However, commonly used trajectory datasets such as ETH, UCY, and GC (Pellegrini et al., 2009; Lerner et al., 2007; Robicquet et al., 2016; Yi et al., 2015) have trajectory recordings less than an hour, which makes it challenging to represent the variety of situations pedestrians encounter. On the other hand, the ATC dataset records the trajectories of people moving around a 900 m^2 shopping mall over 92 days, providing an extensive human trajectory dataset (Bršćić et al., 2013). Consequently, we analyze the ATC dataset to derive the social zone.

As illustrated in Fig.1, the ATC dataset provides pedestrian trajectories across a broad area of the shopping mall. We specifically extracted data from the central square, considering only situations where two individuals encounter each other in a large open space unaffected by walls or other structures. Among the 92 days of recorded data, there were occasions when events held in the square hindered the availability of open space, and such instances were manually removed from the dataset. According to Kitazawa and Fujiyama (2009), people avoid obstacles within a 1 m by 4.5 m range in their direction of gaze. To obtain comprehensive trajectories where people encounter and avoid others from various angles, we defined a larger attentional space of 4 m by 5 m . We extracted data where: 1) the attentional space is contained within the rectangular central square area, 2) only one other pedestrian is present in this space for a duration of 3 seconds, 3) the other pedestrian is initially at least 1 m away, and 4) the reference pedestrian is moving at a speed of at least 0.4 m/s . We collected trajectories of two individuals’ interactions, either walking in the same direction or passing each other, as shown in Fig.2.

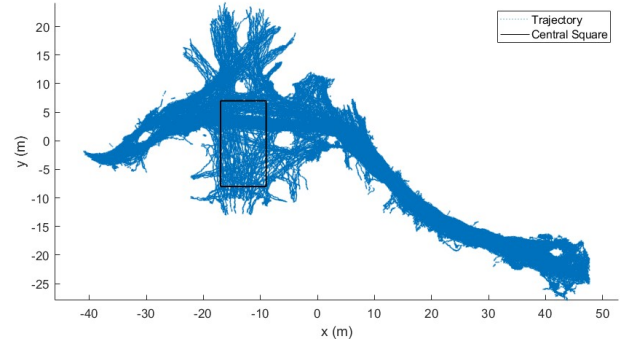


Fig. 1. Pedestrian trajectories in the ATC shopping mall. From this, we can infer the mall’s layout and navigable spaces. The central square has a large open space and exhibits low pedestrian density, which is appropriate for investigating human interactions.

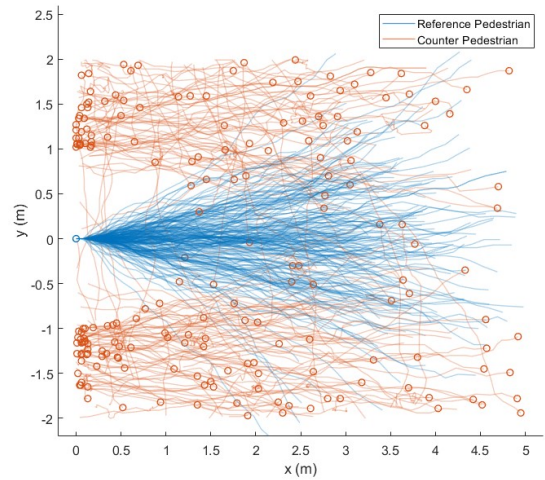
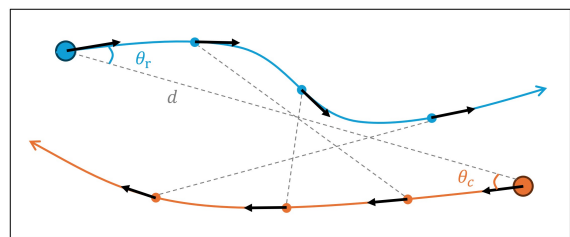


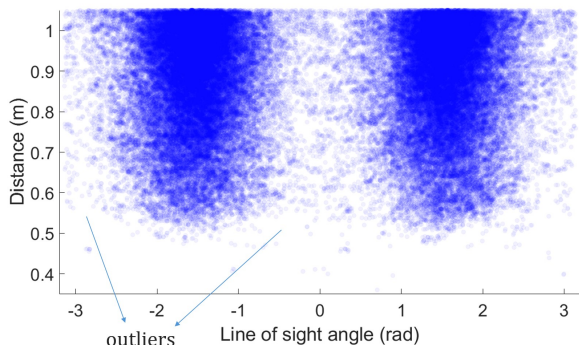
Fig. 2. Examples of processed trajectories of two-person interactions from the open space. Since the data has been collected over an extended period, we can obtain trajectory scenarios of two individuals encountering each other from various speeds and directions. Although this shows 200 example trajectories, we have gathered a total of 16,181 trajectories.

To derive social zones, we use the distance and line of sight (LOS) angle to other pedestrians at each moment. Figure 3 shows these distances according to LOS angles, providing rough information about minimum maintained distances between two pedestrians. Since the data is derived from the real world, outliers may occur, so we need to determine the minimum social zone that aligns with most situations. To remove outliers, we used the Local Outlier Factor (LOF) (Breunig et al., 2000), which operates based on local reachability density. Given the nature of LOF, where data density is low at the boundaries, it may be misclassified as an outlier. To prevent this, we defined the maximum distance in the data as $r_{\max} = 2[m]$, then calculated a complementary distance $r' = r_{\max} - r$. The complementary distance according to angle can be represented in Cartesian coordinates, and we remove the outliers assuming an outlier fraction of 0.2% .

We can represent the data in 3D by adding the instantaneous speed of the reference pedestrian and determine the data’s boundary by constructing a convex hull that encompasses all data points. The 3D convex hull generates a 2D polygon at the



(a) LOS angle and distance between each pedestrian



(b) Correlation between LOS angle and distance

Fig. 3. All distances based on the LOS angle derived from the discrete trajectories of two individuals. This roughly indicates the minimum social distance required for each angle of encounter. Given that this data comes from real-world observations, it may contain noise and outliers. Our goal is to establish the minimum boundary for the majority of the data.

intersection with a plane defined by the speed axis, from which we can derive the minimum social zone according to the speed of the reference pedestrian. To simplify the representation of the minimum social zone depicted by the polygon, we have used minimum enclosing ellipse fitting to represent it as an ellipse (Gärtner and Schönherr, 1997). The obtained social zone is shown in Fig.4.

3. SAFETY-GUARANTEED CONTROLLER

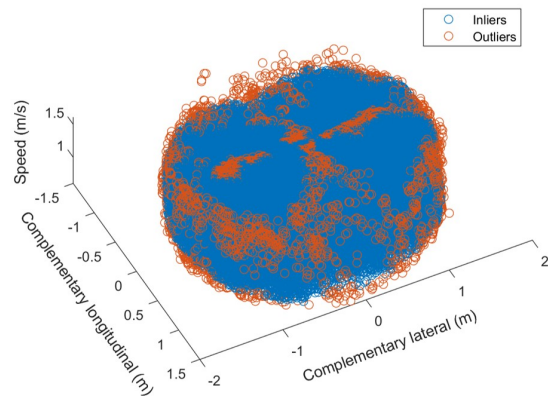
To control robots without invading the obtained minimum social zone, we utilize CBFs (Ames et al., 2019). The safety set S can be defined through a differentiable and continuous barrier function $h(\mathbf{x})$ as $S = \{\mathbf{x} \in \mathbb{R}^n : h(\mathbf{x}) \geq 0\}$. By designing a controller that ensures the barrier function remains positive, the system's trajectory can always reside within the safety set. In a discrete dynamic system model $\mathbf{x}_{k+1} = f(\mathbf{x}_k, \mathbf{u}_k)$, a suitable barrier function can be achieved if there exists a class \mathcal{K} function γ ,

$$\Delta h(\mathbf{x}_k, \mathbf{u}_k) \geq -\gamma h(\mathbf{x}_k), \quad (1)$$

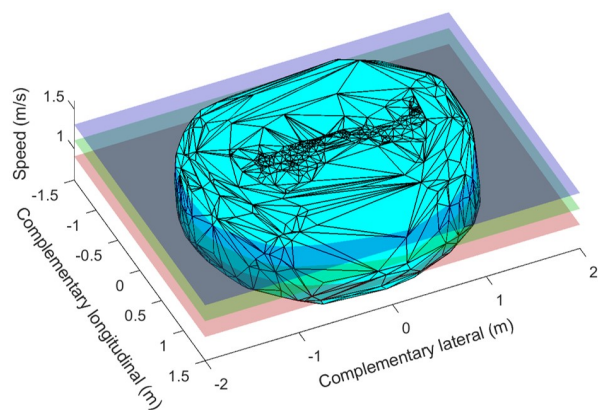
where $\Delta h(\mathbf{x}_k, \mathbf{u}_k) := h(\mathbf{x}_{k+1}) - h(\mathbf{x}_k)$.

To simplify the problem, we use a scalar gamma where $0 < \gamma \leq 1$, and the lower bound of the control barrier function $h(\mathbf{x}_k)$ diminishes exponentially at a rate of $1 - \gamma$.

We are addressing the problem of avoiding the social zones of humans, so it is necessary to reflect the dynamic behaviors of people in the CBF. While it is possible to define and incorporate the state of an obstacle in the system model, we do not know the exact dynamics model of the human, nor can we control it. Additionally, the increased complexity of the state and dynamics model can significantly increase the complexity



(a) Inliers and outliers within the dataset.



(b) Convex hull enclosing the dataset and its intersections at different speeds.

Fig. 4. The distance data according to the reference pedestrian's speed, along with the dataset's outliers and enclosing convex hull. The distance dataset is represented through the complementary distance r' to eliminate outliers effectively. In this case, the problem of finding the minimum distance according to the LOS angle is transformed into finding the maximum, making it easier to identify outliers and construct a convex hull that encompasses all the data.

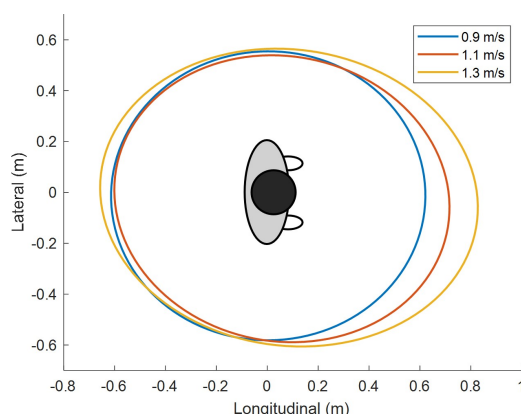


Fig. 5. Estimated minimum social zones according to pedestrian speed from the ATC dataset. These exhibit an asymmetrical shape, with a shorter distance on the left.

of optimization. To address this, we can consider roughly predicting the movements of humans and integrating this with the MPC framework (Zeng et al., 2021). MPC optimizes control

inputs iteratively based on model predictions, demonstrating robustness against noise or situation variations.

(MPC-CBF) Find $\mathbf{u}_k \in \mathcal{U}$ such that

$$\begin{aligned} \min_{\mathbf{u}_k} \quad & \mathbf{x}_N^\top P \mathbf{x}_N + \sum_{k=1}^{N-1} \mathbf{x}_k^\top Q \mathbf{x}_k + \mathbf{u}_k^\top R \mathbf{u}_k \\ \text{s.t.} \quad & \mathbf{x}_{k+1} = f(\mathbf{x}_k, \mathbf{u}_k) \\ & \mathbf{x}(0) = \mathbf{x}_0, \quad \mathbf{x}_k \in \mathcal{X}_k, \quad \mathbf{u}_k \in \mathcal{U}_k, \quad k = 0, 1, \dots, N-1 \\ & \Delta h(\mathbf{x}_k, \mathbf{u}_k) \geq -\gamma h(\mathbf{x}_k), \quad k = 0, 1, \dots, N_h - 1 \end{aligned} \quad (2)$$

where $\mathcal{X} \subset \mathbb{R}^n$ and $\mathcal{U} \subset \mathbb{R}^m$ are the feasible state and control input sets, N and N_h are the length of the prediction horizon for MPC and CBF constraints, and P , Q , and R are semi-positive definite cost matrices.

For the barrier function, it should satisfy $h(\mathbf{x}) = 0$ at the safe boundary and $h(\mathbf{x}) > 0$ within other safe areas. Furthermore, an ideal barrier function would possess symmetry depending on the direction, ensuring it does not exhibit any particular bias toward being too evasive or close. In other words, when defined as a function influenced only by the distance from the boundary, $h(\mathbf{x}) = h(\mathbf{x}_r, \mathbf{x}_o) = h(d(\mathbf{x}_r, \mathbf{x}_o))$, where d is the distance function between the states of the robot \mathbf{x}_r and the obstacles \mathbf{x}_o , it enables consistent control to maintain distances regardless of the obstacle's shape. We assume that the general obstacle can be represented as line segments and use the following approximated distance function (Shapiro and Tsukanov, 1999). Let the endpoints of the line segment be $\mathbf{x}_a = (x_a, y_a)$ and $\mathbf{x}_b = (x_b, y_b)$, the length $L = \|\mathbf{x}_a - \mathbf{x}_b\|$, and the midpoint $\mathbf{x}_c = (\mathbf{x}_a + \mathbf{x}_b)/2$. We define:

$$g(\mathbf{x}) := [(x - x_a)(y_b - y_a) - (y - y_a)(x_b - x_a)]/L, \quad (3)$$

which is the signed distance function from point \mathbf{x} to the line passing through \mathbf{x}_a and \mathbf{x}_b .

A line segment can be represented as the intersection of an infinite line and a trimming region, such as a circular disk. We consider the following trimming function that is normalized to first order:

$$t(\mathbf{x}) = \frac{1}{L} [(L/2)^2 - \|\mathbf{x} - \mathbf{x}_c\|^2]. \quad (4)$$

With $g(\mathbf{x})$ and $t(\mathbf{x})$, a normalized distance function for the line segment,

$$d(\mathbf{x}) = \sqrt{g(\mathbf{x})^2 + (\|t(\mathbf{x})\| - t(\mathbf{x}))^2/4}, \quad (5)$$

is zero exactly on the points of the line segment, positive everywhere else.

For an elliptical social zone, we define the distance function as a sum of distances from the two foci of the ellipse based on the fact that the sum of the distances from any point on the ellipse to two foci is constant. This provides an adequate approximation when the distance between the two foci of the ellipse is not too large. A general ellipse equation that is rotated by an angle θ , centered at (m, n) with a and b as the semi-major and semi-minor axes respectively, is given by:

$$\begin{aligned} & [(x - m) \cos(\theta) + (y - n) \sin(\theta)]^2/a^2 \\ & + [(x - m) \sin(\theta) + (y - n) \cos(\theta)]^2/b^2 = 1. \end{aligned} \quad (6)$$

The foci are located at $\mathbf{c}_a = (m + c \cos(\theta), n + c \sin(\theta))$ and $\mathbf{c}_b = (m - c \cos(\theta), n - c \sin(\theta))$ where $c = \sqrt{a^2 - b^2}$, and the distance function is defined as follows:

$$d(\mathbf{x}) = (\|\mathbf{x} - \mathbf{c}_a\| + \|\mathbf{x} - \mathbf{c}_b\|)/2 - a. \quad (7)$$

4. SIMULATION RESULTS

In simulations, we demonstrate that the robot avoids a human using a minimum social zone and an MPC-CBF controller. We use a simple 2D double integrator model to describe the robot's dynamics:

$$\mathbf{x}_{k+1} = \begin{bmatrix} 1 & 0 & \Delta t & 0 \\ 0 & 1 & 0 & \Delta t \\ 0 & 0 & 1 & 0 \\ 0 & 0 & 0 & 1 \end{bmatrix} \mathbf{x}_k + \begin{bmatrix} 0.5(\Delta t)^2 & 0 \\ 0 & 0.5(\Delta t)^2 \\ \Delta t & 0 \\ 0 & \Delta t \end{bmatrix} \mathbf{u}_k, \quad (8)$$

where $\mathbf{x}_k = \{x, y, v_x, v_y\}$, $\mathbf{u}_k = \{f_x, f_y\}$, and Δt is the time step.

It is assumed that the human moves at a constant speed of 0.5 m/s and is unaffected by the robot's movements. The robot is assumed to have accurate knowledge of the human's position and velocity. The robot's maximum speed has been set at 1 m/s , and accordingly, it has been configured to always maintain a social zone of 1.1 m/s . The robot is modeled as a cylindrical shape with a radius $r_r = 0.5 \text{ m}$, and a barrier function is designed to be greater than the robot's radius. However, since the approximated distance function contains some errors, an additional small margin has been set $\epsilon = 0.05$, $h(\mathbf{x}) = d(\mathbf{x}) - r_r - \epsilon \geq 0$. The implementation of MPC-CBF utilizes the code from Zeng et al. (2021), and optimization was performed using the IPOPT (Wächter and Biegler, 2006) solver.

The simulation was conducted with a 0.1-second time step interval (Δt), with the MPC's prediction horizon (N) set at 8, and the CBF's horizon (N_h) at 2. Despite having a shorter horizon than MPC, CBF can ensure stability, thereby increasing computational efficiency.

We investigate the robot's behavior in the following scenarios:

- (1) Passing by a person facing directly;
- (2) Avoiding an approaching person in a narrow corridor;
- (3) Encountering a person in a restricted pathway.

The third scenario shows two different cases depending on the positions of the robot and person. The results for these scenarios are depicted in Fig. 6.

Each scenario demonstrates that the robot can appropriately follow social norms while avoiding humans. In Fig. 6a, when directly facing a person, the robot maneuvers to the right. This adheres to the common practice of passing on the right when people meet face-to-face. This action results from the learned minimum social zone being larger on the right side, mirroring the observed behavior that people generally leave more space on their right side while passing others. We conjecture that adhering to the social norm of passing on the right creates a feeling of comfort even in narrower spaces, but breaking this norm by avoiding someone to the left typically results in moving further away to maintain distance.

In Fig. 6b, the robot is observed to reduce its speed when avoiding an approaching person in a narrow pathway. This is due to the CBF controller's feature. As the robot nears the safety boundary, the controller automatically slows the robot to enhance stability and prevent collisions. This cautious approach not only prevents collisions with walls and avoids intruding into the person's minimum social zone but also reassures humans of

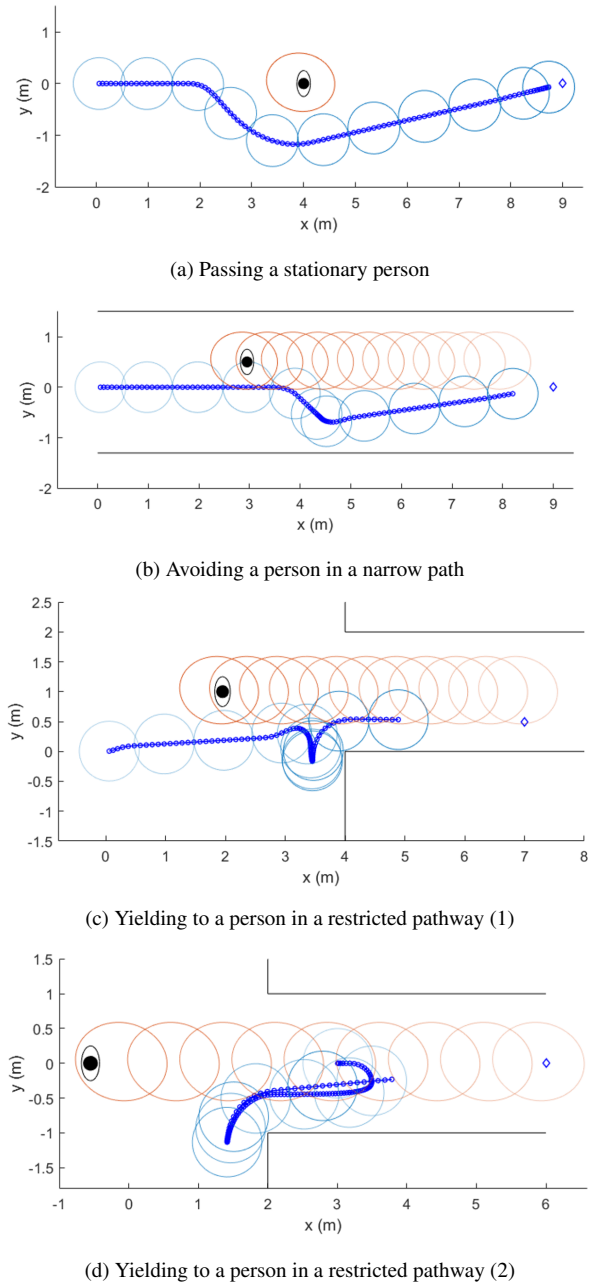


Fig. 6. Robot and human interaction scenarios in various pathway conditions. The human’s social zone is shown as a red ellipse, and the robot as a blue circle, with colors deepening over time to indicate progression. The robot’s path is marked by circular markers. It targets a blue diamond, while a black line represents an obstructive wall.

their safety by demonstrating that the robot will not cause harm, thereby providing a sense of comfort.

The results of scenario 3 in Fig. 6c and 6d, illustrate the robot’s behavior strategies, to allow a person to pass by waiting or creating sufficient space before it proceeds. It is preferable for the robot to give priority to human movement. By yielding to humans, the robot not only empowers them to make decisions but also facilitates adaptable responses to unexpected situations, thereby enhancing safety. Moreover, this deference creates an environment where people can behave more naturally and autonomously, promoting a harmonious and effective

integration of robotic systems into social settings. The degree to which the robot yields can be adjusted by varying the size of the social zone, allowing us to appropriately trade off between the robot’s yielding behavior and navigation efficiency.

5. DISCUSSION

A major challenge in social robot navigation is the difficulty of explicitly defining objectives or cost functions. Reinforcement learning and imitation learning have been employed to derive socially compliant behaviors from simulations or real human trajectories (Kretzschmar et al., 2016; Möller et al., 2021). However, these approaches tend to replicate human behavior policies without adequately explaining how they conform to social norms. In this study, by clearly defining the social zone and incorporating it into the control framework, we can better understand, fine-tune, and adapt the process to various situations. Additionally, the use of CBF ensures safety, which is practically advantageous over learning-based policies.

As shown in the simulation results, the integration of the social zone and CBF not only allows for avoidance based on learned human social norms but also promotes socially considerate behaviors such as slowing down or yielding. However, these behaviors vary depending on the CBF’s barrier function and the controller’s parameters because the defined minimum social zone only specifies the safety boundary at $h(\mathbf{x}) = 0$ and does not dictate behaviors outside this boundary. Future research could extend to defining the barrier function for regions where $h(\mathbf{x}) > 0$, and developing controllers using CBF that mimic human-like avoidance maneuvers.

Furthermore, as our results have shown, the minimum social zone changes depending on the agent’s speed. This can be further influenced by various factors, including environmental context, proximity to obstacles, population density, and diverse types and behaviors of people. Although our simulations assumed a constant social zone for optimization, recognizing and incorporating the variability in social zones with speed could enable the creation of control policies better tailored to specific environmental and social conditions.

6. CONCLUSION

In this research, we have introduced a novel approach to socially compliant robot navigation by incorporating real-world human social zones into a robotic control system. Utilizing extensive real-life data, our method effectively addresses both physical and psychological aspects of human-robot interactions. Additionally, it extends to a navigation system that employs CBF and MPC to ensure safety amidst dynamic obstacles. Simulation results demonstrate that our approach enables the robot to adjust its behavior—like modulating speed, pausing, and yielding—showing strong potential for practical application. Moreover, identifying social zones deepens our understanding of space and human movement, crucial in human-centric environments.

REFERENCES

- Ames, A.D., Coogan, S., Egerstedt, M., Notomista, G., Sreenath, K., and Tabuada, P. (2019). Control barrier functions: Theory and applications. In *2019 18th European control conference (ECC)*, 3420–3431. IEEE.

- Breunig, M.M., Kriegel, H.P., Ng, R.T., and Sander, J. (2000). Lof: identifying density-based local outliers. In *Proceedings of the 2000 ACM SIGMOD international conference on Management of data*, 93–104.
- Bršćić, D., Kanda, T., Ikeda, T., and Miyashita, T. (2013). Person tracking in large public spaces using 3-d range sensors. *IEEE Transactions on Human-Machine Systems*, 43(6), 522–534.
- Corbetta, A., Meeusen, J.A., Lee, C.m., Benzi, R., and Toschi, F. (2018). Physics-based modeling and data representation of pairwise interactions among pedestrians. *Physical review E*, 98(6), 062310.
- Francis, A., Pérez-d’Arpino, C., Li, C., Xia, F., Alahi, A., Alami, R., Bera, A., Biswas, A., Biswas, J., Chandra, R., et al. (2023). Principles and guidelines for evaluating social robot navigation algorithms. *arXiv preprint arXiv:2306.16740*.
- Fu, B., Kathuria, T., Rizzo, D., Castanier, M., Yang, X.J., Ghaffari, M., and Barton, K. (2023). Human-robot matching and routing for multi-robot tour guiding under time uncertainty. *arXiv preprint arXiv:2309.15373*.
- Gärtner, B. and Schönherr, S. (1997). Smallest enclosing ellipses: fast and exact.
- Gérin-Lajoie, M., Richards, C.L., Fung, J., and McFadyen, B.J. (2008). Characteristics of personal space during obstacle circumvention in physical and virtual environments. *Gait & posture*, 27(2), 239–247.
- Hall, E.T. (1963). A system for the notation of proxemic behavior. *American anthropologist*, 65(5), 1003–1026.
- Hayduk, L.A. (1981). The shape of personal space: An experimental investigation. *Canadian Journal of Behavioural Science/Revue canadienne des sciences du comportement*, 13(1), 87.
- Kathuria, T., Xu, Y., Chakhachiro, T., Yang, X.J., and Ghaffari, M. (2022). Providers-clients-robots: Framework for spatial-semantic planning for shared understanding in human-robot interaction. In *2022 31st IEEE International Conference on Robot and Human Interactive Communication (RO-MAN)*, 1099–1106. IEEE.
- Kirby, R., Simmons, R., and Forlizzi, J. (2009). Companion: A constraint-optimizing method for person-acceptable navigation. In *RO-MAN 2009-The 18th IEEE International Symposium on Robot and Human Interactive Communication*, 607–612. IEEE.
- Kitazawa, K. and Fujiyama, T. (2009). Pedestrian vision and collision avoidance behavior: Investigation of the information process space of pedestrians using an eye tracker. In *Pedestrian and evacuation dynamics 2008*, 95–108. Springer.
- Korbmacher, R. and Tordeux, A. (2022). Review of pedestrian trajectory prediction methods: Comparing deep learning and knowledge-based approaches. *IEEE Transactions on Intelligent Transportation Systems*, 23(12), 24126–24144.
- Kretschmar, H., Spies, M., Sprunk, C., and Burgard, W. (2016). Socially compliant mobile robot navigation via inverse reinforcement learning. *The International Journal of Robotics Research*, 35(11), 1289–1307.
- Lerner, A., Chrysanthou, Y., and Lischinski, D. (2007). Crowds by example. In *Computer graphics forum*, volume 26, 655–664. Wiley Online Library.
- Mavrogiannis, C., Baldini, F., Wang, A., Zhao, D., Trautman, P., Steinfeld, A., and Oh, J. (2023). Core challenges of social robot navigation: A survey. *ACM Transactions on Human-Robot Interaction*, 12(3), 1–39.
- Möller, R., Furnari, A., Battiato, S., Härmä, A., and Farinella, G.M. (2021). A survey on human-aware robot navigation. *Robotics and Autonomous Systems*, 145, 103837.
- Neggers, M.M., Cuijpers, R.H., Ruijten, P.A., and IJsselsteijn, W.A. (2022a). Determining shape and size of personal space of a human when passed by a robot. *International Journal of Social Robotics*, 14(2), 561–572.
- Neggers, M.M., Cuijpers, R.H., Ruijten, P.A., and IJsselsteijn, W.A. (2022b). The effect of robot speed on comfortable passing distances. *Frontiers in Robotics and AI*, 9, 915972.
- Patompak, P., Jeong, S., Nilkhamhang, I., and Chong, N.Y. (2020). Learning proxemics for personalized human-robot social interaction. *International Journal of Social Robotics*, 12, 267–280.
- Pellegrini, S., Ess, A., Schindler, K., and Van Gool, L. (2009). You’ll never walk alone: Modeling social behavior for multi-target tracking. In *2009 IEEE 12th international conference on computer vision*, 261–268. IEEE.
- Pouw, C.A., Corbetta, A., Gabbana, A., van der Laan, C., and Toschi, F. (2024). High-statistics pedestrian dynamics on stairways and their probabilistic fundamental diagrams. *Transportation research part C: emerging technologies*, 159, 104468.
- Rios-Martinez, J., Spalanzani, A., and Laugier, C. (2015). From proxemics theory to socially-aware navigation: A survey. *International Journal of Social Robotics*, 7, 137–153.
- Robicquet, A., Sadeghian, A., Alahi, A., and Savarese, S. (2016). Learning social etiquette: Human trajectory understanding in crowded scenes. In *European conference on computer vision*, 549–565. Springer.
- Shapiro, V. and Tsukanov, I. (1999). Implicit functions with guaranteed differential properties. In *Proceedings of the fifth ACM symposium on Solid modeling and applications*, 258–269.
- Svenstrup, M., Bak, T., and Andersen, H.J. (2010). Trajectory planning for robots in dynamic human environments. In *2010 IEEE/RSJ International Conference on Intelligent Robots and Systems*, 4293–4298. IEEE.
- Teng, S., Gong, Y., Grizzle, J.W., and Ghaffari, M. (2021). Toward safety-aware informative motion planning for legged robots. *arXiv preprint arXiv:2103.14252*.
- Truong, X.T. and Ngo, T.D. (2016). Dynamic social zone based mobile robot navigation for human comfortable safety in social environments. *International Journal of Social Robotics*, 8, 663–684.
- Wächter, A. and Biegler, L.T. (2006). On the implementation of an interior-point filter line-search algorithm for large-scale nonlinear programming. *Mathematical programming*, 106, 25–57.
- Wkas, J., Gudowski, B., and Matuszyk, P.J. (2006). Social distances model of pedestrian dynamics. In *Cellular Automata: 7th International Conference on Cellular Automata, for Research and Industry, ACRI 2006, Perpignan, France, September 20-23, 2006. Proceedings 7*, 492–501. Springer.
- Yi, S., Li, H., and Wang, X. (2015). Understanding pedestrian behaviors from stationary crowd groups. In *Proceedings of the IEEE conference on computer vision and pattern recognition*, 3488–3496.
- Zeng, J., Zhang, B., and Sreenath, K. (2021). Safety-critical model predictive control with discrete-time control barrier function. In *2021 American Control Conference (ACC)*, 3882–3889. IEEE.